ARID ZONE JOURNAL OF ENGINEERING, TECHNOLOGY & ENVIRONMENT
AZOJETE June 2025. Vol.21(2):431-448
Published by the Faculty of Engineering, University of Maiduguri, Maiduguri, Nigeria.
Print ISSN: 1596-2490, Electronic ISSN: 2545-5818
https://doi.org/10.63958/AZOJETE/2025/21/02/010
www.azojete.com.ng

ORIGINAL RESEARCH ARTICLE

ASSESSMENT OF VEGETATION LOSS AND LAND SURFACE TEMPERATURE CHANGES IN BWARI AREA COUNCIL, ABUJA NIGERIA

K. J. Ekanem[1] and A. Bukuromo[2]*

[1]Department of Survey, GIS and Mapping, NALDA, Abuja Nigeria
[2]Department of Civil Engineering, Federal University Otuoke, Bayelsa State, Nigeria
Corresponding author's email: preaye@gmail.com

ARTICLE INFORMATION

Received: 23rd February 2025
Revised: 24th March 2025
Accepted: 24th March 2025

Keywords:
Geospatial
Normalized difference vegetation index
Land surface emissivity
Normalized difference building index (NDBI)

ABSTRACT

Urban vegetation is one of the key essential components that contributes to ecological balance and environmental sustainability. However, due to rapid urbanization in the last few decades, there has been cases of vegetation loss which has increased the land surface temperature (LST) and affected the environmental sustainability. Thus, the aim of this study is assessing the impact of vegetation loss on Land Surface Temperature of Bwari Area Council during the periods of 1990-2021, using geospatial techniques. The support vector machine (SVM) supervised classification algorithm was used to classify Satellite imageries into land use land cover (LULC) maps according into buildup area, water body, vegetation and rock/bare ground using ArcGIS Pro. All the classified LULC maps had an overall accuracy of more than 90% with the overall Kappa coefficient also more than 0.9. The analysis of LULC estimation suggests a significant increase in Built-up areas (+ 255.45%) and a reduction in Vegetated areas (-75.17 %) from 1990 to 2021. Brightness temperature, Land Surface Emissivity (LSE) and Normalized Difference Vegetation Index (NDVI) were computed to estimate land surface temperature. The results show that the LST was higher in the regions of built-up areas and rock/bare ground but lower in vegetated areas with the maximum temperature of the study area increasing from 37.11 °C in 1990 to 58.87 °C in 2021. Correlation between land surface temperature and NDVI/NDBI for the study periods was carried out. The results show that correlations between NDVI and LST are rather weak negative, but there is a strong positive correlation between NDBI and LST. These results call for implementation of policies to control rapid urban growth in Bwari Area Council and preserve vegetal covers and as well an extension of the implementation of the Abuja Master Plan to Satellite Towns around Abuja.

1.0 Introduction

Rapid population growth entails high demand for social, economic and industrial infrastructure and this results in unplanned and uncoordinated urbanization, particularly in developing countries around the world. In many instances, urban development takes place at the expense of vegetated areas (Kafy et al., 2021) which leads to dramatic changes in the local microclimatic condition of several urban locations(Chibuike et al., 2018). There is great threat to forest cover aand the broader domain of vegetative cover on the land surface and the main source is humans through urbanization (Waseem & Khayyam, 2019). While urbanization can be said to be an indication of economic growth and success, it has also brought about short and long-term negative implications in cities' development (Maimaitiyiming *et al.*, 2014). The process of urbanization has brought about several undesirable environmental consequences such as flooding (Santamouris, 2014), air pollution (Anker *et al.*, 2019), and even heat related morbidityy.Ullah *et al.*, (2019), noticed that rapid urbanization has unfortunately led to changes in existing patterns of land use land cover (LULC) globally, and this has consequently increased the land surface temperature (LST) in many regions (Wang *et al.*, 2018; Ayanlade & Howard, 2019; Ullah *et al.*, 2019; Kafy *et al.*, 2021). Several studies have found that the conversion of marsh, vegetative, and agricultural lands into built-up areas is hastened by urbanization and the subsequent catalysts for LULC change, which inadvertently drives up the cities' LST (Tran et al., 2006 Arsiso *et al*., 2018; Kafy *et al*., 2021;). In these studies, the rise in land surface temperature is seen as a long-term consequence of LULC change particularly in Urban Areas (UAs).

Factors contributing to Urban Heat Island (UHI) effects include urban ecology (less vegetation cover, thus reduced cooling from evapotranspiration), engineered building material properties (higher thermal capacity and storage), anthropogenic heat emissions (vehicular traffic and heating/cooling of built infrastructure), hydrological changes (increased runoff due to impervious surfaces and heat transmitted to streams via urban runoff), and urban canyon geometry (reduction of outgoing radiative heat flux due to 'heat trapping' in street canyons) (Sharma *et al*., 2016). Also, variables like smart urban growth consisting of both vertical and horizontal expansion, construction materials, the distance between buildings, locations of public spaces, roads, bus stops, major and minor industrial hubs, and so on, have a direct impact on temperature concentration in the cities (Ahmed *et al*., 2013; Chen *et al.,* 2020; Kafy *et al*., 2021)

In addition to considerable land use/land cover (LULC) vegetation loss, rapid urban growth also contributes to an imbalance between demand and supply, thus making available infrastructure to be under stress and as a result altering urban climate (Mahmoud & Gan, 2018). There is usually increased demand for housing, roads, power generation and feeding etc. To meet these demands, fractions of vegetation and green spaces is reduced leading to subsequent inhibition of photosynthetic activity and plant's water transpiration biodiversity is threatened and this affects ecosystem productivity through the gradual but consistent loss of habitat, biomass and carbon storage (Seto *et al.,* 2012).

Increasing or conserving green infrastructure in cities has thus been proposed by several authors as a strategy to regulate high temperatures (Oliveira *et al*. 2011; Norton *et al*. 2015). These green infrastructures or vegetated surfaces, such as green walls and roofs, parks, gardens, green spaces, lawns, and trees, is said to capture solar radiation to different extents and ultimately reduce the Urban Heat Island effects (Bowler *et al*. 2010). Also, Oliveira *et al*. (2011) examined the cooling effects of vegetated, urban spaces in Portugal and subtropical China and found it to be effective.

Di Leo *et al*, (2016) studied the role of urban green infrastructure in mitigating land surface temperature in Bobo-Dioulasso, Burkina Faso, and found that Land Surface Temperature in green infrastructure areas was indeed lower than adjacent impervious, urbanized areas. In the same vein, in Nigeria, in assessing the impact of green parks cooling effect on Abuja urban microclimate, Chibuike *et al*.(2018) noted the need for urban planners to design green spaces with stronger cooling effects along with the city designing, to mitigate UHI phenomenon. This is further buttressed by studies carried out in Ibadan by (Balogun & Daramola, 2019) where it was posited that the most efficient approach for UHI mitigation is the increase in urban green spaces and parks as this results in less solar radiation absorption through shading of the land surface. However, even though this mitigative measures are being put in place in these areas, there are still high loss of vegetation or vegetative cover in many areas without replacement of such and this has led to a significant increase in the land surface temperature in these places. Therefore, this research aimed to assess the impacts of vegetation loss on land surface temperature of Bwari Area Council, in the Federal Capital Territory.

i. To assess the changes in landuse/landcover that has occurred between 1990-2001 and 2001-2021 in the study area;
ii. To assess the spatio-temporal changes in land surface temperature in the study area between 1990-2001 and 2001-2021 and
iii. Examine the relationship between vegetation loss in the period under study and the spatio-temporal changes in land surface temperature in the study area.

1.1 Study Area

1.1.1 Location and administration

The Bwari Area Council is one of the six (6) area councils in the Federal Capital Territory (FCT), located within Longitudes 7°10' and 7°45'East, and Latitudes 8° 50' and 9° 30' North (Figure 1). It lies in the north – eastern part of the Federal Capital Territory. Bwari Area Council is bounded in the north by Kagarko in Kaduna State, in the east by Karu in Nassarawa State, in the south by AMAC in FCT and bounded in the west by Suleja and Tafa, all in Niger State. It is the second most populous area council after Abuja Municipal Council (AMAC) with a population of 581,100 according to National Population Commission's 2016 population projection (National Population Commission, 2016).

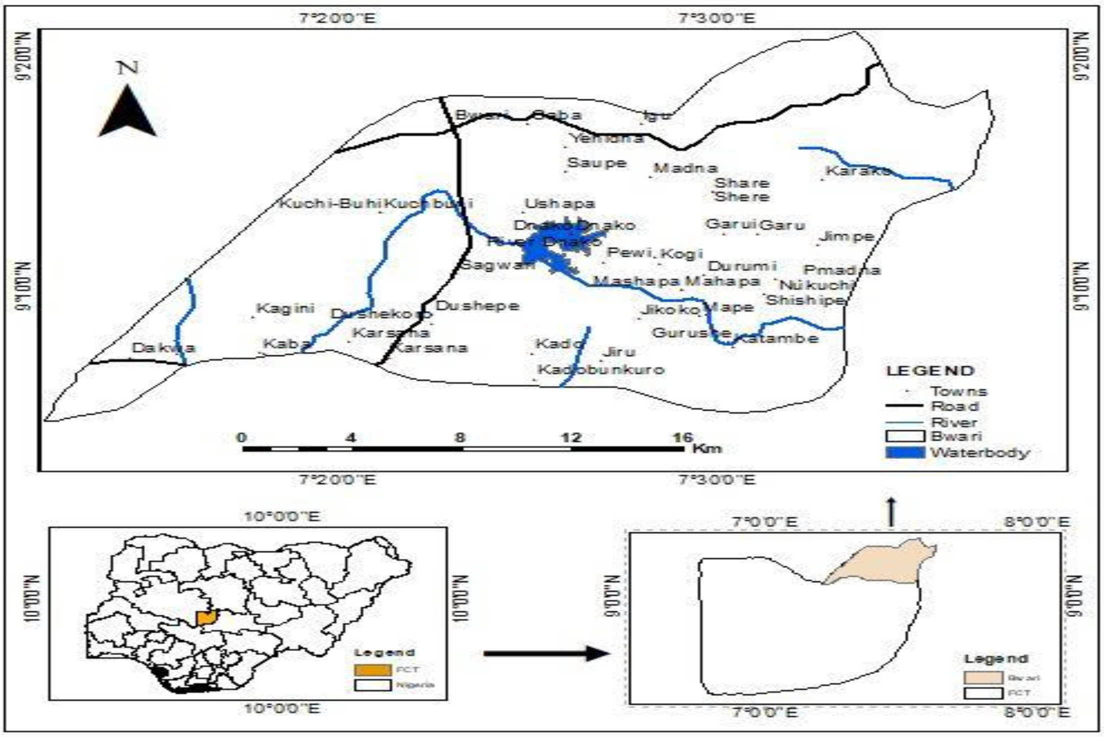

Figure 1: The Study Area: Bwari Area Council

1.1.2 Climate and relief

Bwari has a climate classified by Koppen as tropical wet and dry (Aw). The area experiences two seasons annually (Edicha & Mgbanyi, 2013; Igun & Williams, 2018). These are warm, humid rainy season and a cold dry season. Fortunately, the high altitudes and undulating terrain of the study area, act as moderating influence on the weather of the territory. The rainy season begins from April and ends in October, with September being the peak of the rainy season and due to the hilly and mountainous nature of the study area, orographic activities bring heavy and frequent rainfall of about 1500 mms (59.1 in) during the rainy season (Awuh *et al*., 2019).

The study area falls within the Savannah zone vegetation of the West African sub-region and is divided into three Savannah types namely; Grassy, Savannah woodland and Shrub Savannah (Rakiya. *et al*., 2018). The soil in the area is basically alluvial and luvisols making it a fertile ground for agriculture and vegetation growth (Awuh *et al*., 2019).

The Area Council features an interesting terrain, which combines rounded hills and clusters of rock outcrops dissected by river valleys, as well as gentle rolling plains. It falls within the Abuja hills and dissected zone of the Jema'a Platform. Generally viewing the study area, the hilly areas are found towards the eastern part, posing constraint to physical development while the plains occupy the central and western areas. The study area is the highest part of the FCT with several peaks that are about 760 meters above sea level. The lower Usuma dam which provides portable water for the whole FCT (Wuana *et al*., 2020), is located in the study area. Bwari Area Council is also home to a lot of quarry sites and this explains why they appear to be areas of temperature hot zones in the study area even where there is vegetation around. The main land use types in the study area include built-up, residential, commercial, institutional, administrative, roads and industrial settlements. Bwari houses major government establishments like the Joint Admission and Matriculation Board (JAMB) Headquarters, the Abuja Law School, General Hospital, Dorben Polytechnic, Veritas University and other private, commercial and industrial establishments. These establishments have so far led to the increase in population and as such resulting in significant loss of vegetation during the study period in order to accommodate more housing units and significant degree of urbanization. These changes have had an impact on the local climate of the area, particularly, the land surface temperature of the area, which forms the focus of this research.

2. Materials and Method

2.1 Overview of Approach

For data analysis to answer the research questions, Geographic Information System (GIS) and Remote Sensing (RS) methods were deployed for data processing and results generation. The use of GIS and Remote Sensing was backed up by the fact that these tools assist for capturing, storing, manipulating and analyzing of the data USGS server and NIMET served as sources of the Landsat data and temperature data respectively, used for the analysis for the research.

2.2 Data Source

This research utilized Landsat 5, Landsat 7 and Landsat 8 satellite imageries with path/row 189/54, sourced from the United State Geological Survey (USGS) server, while the local government boundary map for delineating the spatial extent of the study area and Nigerian Administrative map was obtained as a shape file from Office of the Surveyor General (OSGOF). For LST validation purpose and, temperature data from NIMET for the study area and period were used. The choice of Landsat satellite imageries was the presence of the thermal bands for the use of the calculation of land surface temperature (Hami *et al*., 2019; Sekertekin & Bonafoni, 2020).

Table 1 is the tabular presentation of the data sources while Table 2 is the description of the Landsat data used for the study.

Table 1: Data Source

S/N	Data Type	Year	Source
1	Landsat 5,7 and 8	1990,2001 and 2021	USGS
2	Insitu temperature data	1990,2001 and 2021	NIMET
3	Boundary shape file of study area		OSGOF

Table 2: Description of Landsat Data used for the study.

Sensor Sensor	No of Bands	Resolution	Path/Row	Date	Significance
Landsat **Landsat 5** TM	6 6	30	189/54	12/02/1990	Used for land cover classification and generation of NDVI/NDBI
TI TIRS(band6)	1	120 Resample 30 120m	189/54	12/02/1990	Used for LST retrieval
Landsat 7 ETM	7 7	30	189/54	09.01/1990	Used for land cover classification and generation of NDVI/NDBI
TIRS (band 6)	1 1	60 Resampled 30	189/54	09/01/2001	Used for LSTretrieval
Landsat 8 OLI	9 9	30	189/54	09/02/2021	Used for land cover classification and generation of NDVI/NDBI
TIRS (band 10 and 11)	2	100 Resampled 30	189/54	09/02/2021	Used for LST retrieval

2.3 *Land* Use/Land Cover Classification

To assess the spatio-temporal changes in physical land types/features (landcover) present in the study area, Landsat imageries covering the study area was extracted and used to produce the Land Use Land Cover maps for Bwari Area Council.

ArcGIS Pro 2.8.4 version was used for the land use land cover classification (LULC) and the algorithm used was the Support Vector Machine (SVM) under the supervised classification method. The SVM is a non-parametric classifier equipped with a set of related learning algorithms used for regression and classification, it places no assumption to the probability distribution of the data and has low training data requirements(Ullah et al., 2019).SVM is among the effective method and chosen for its reliability (Mushore et al., 2017).

The classes are Water body, Vegetation, Built-up Area and Rocks_Bare-ground and samples were taken accordingly create signature files for the SVM algorithm. For the classification of the Landsat 5 and 7 of 1990 and 2001, bands combination of 4-3-2 for false color (infrared), and 5-4-3 for (vegetation analysis) was used to properly classify the imageries. The two band combinations were used to properly identify the different classes of objects present in the imageries. For Landsat 8 of 2021, band combinations of 5-4-3 for false color (infrared) and 654 for false color (vegetation analysis) was used to achieve the same purpose. Google Earth images were used as ground control points (GCPs) to ascertain that the GCPs and the features registered on the Landsat imageries correspond to each other. Thereafter, accuracy assessment was carried out for the land cover classification.

2.4 Accuracy Assessment

Accuracy is done to see how closely the results relate to the true values and gives the qualitative collection of information from the obtained satellite data (Choudhury et al., 2019). To carry out the accuracy assessment of the image classification, the confusion matrix and the kappa index, both considered as one of the best indicators for image classification accuracy (Ullah et al., 2019; Kafy et al., 2021;) were computed using the ArcGIS 10.8. For the accuracy assessment, a total of 208, 207 and 242 reference points were selected on the 1990, 2001 and 2021 composite imageries respectively for the accuracy assessment of the classified LULC maps.

2.5 Normalized Difference Vegetation Index (NDVI) and Normalized Difference Building Index (NDBI)

NDVI is a satellite measured vegetation indices, commonly used to quantify the abundance and energy absorption by leaf pigments such as chlorophyll and is also indicative of an urban climate (Heather *et al*., 2019). It is largely influenced by the fractional cover of the ground by vegetation, the vegetation density and the vegetation greenness. In order words, it indicates the photosynthetic capacity of the land surface cover. Normalized Difference Vegetation Index (NDVI) quantifies vegetation by measuring the difference between near-infrared (which vegetation strongly reflects) and red light (which vegetation absorbs). NDVI is commonly used to quantify the abundance and energy absorption by leaf pigments such as chlorophyll and is also indicative of an urban climate (Bachir *et al*., 2021) . To generate the NDVI for 1990, 2001 and 2021, multi-temporal Landsat visible and near-infrared bands were combined in a normalized ratio using raster calculator in ArcGIS 10.8 to compute the Normalized Difference Vegetation Index. For 1990 and 2001, bands 3(visible red) and 4(near infrared) were used while bands 4(visible red) and 5(near infrared) were used for 2021 imagery. The bands used correspond to the required bands for NDVI calculation for Landsat 5(1990), Landsat 7(2001) and Landsat 8(2021) respectively.

Equally, NDBI, a built-up index commonly used as both an indicator of intensity of development and of urban impervious surface (Macarof & Statescu, 2017), was generated for the 3 years under study. While NDVI is generated using a combination of Landsat near infrared and the red band, NDBI is generated by combining multi-temporal Landsat near-infrared and short-wave infrared bands in a normalized ratio using raster calculator in ArcGIS 10.8. For 1990 and 2001, bands 4(near infrared) and 5(short-wave infrared) are combined while for 2021, bands 5(NIR) and 6(SWIR) using the formula in equation 2.

The following formula was used for NDVI and NDBI calculation

$$NDVI = \frac{(NIR - RED)}{(NIR + RED)} \quad 1$$

$$NDBI = \frac{(SWIR - NIR)}{(SWIR + NIR)} \quad 2$$

Where NIR = Near Infrared, SWIR = Short wave infrared

2.6 Land Surface Temperature (LST) Retrieval

The Land Surface Temperature (LST) was calculated through the use of satellite thermal infrared Remote Sensing system. This is known to provide a synoptic and uniform means of measuring LST at regional scale as compared to in situ sensors of air temperature via weather station networks which is best suited for atmospheric air temperature (Yuan & Bauer, 2007), are sparsely located and the observations being point data, are not a representative of the whole terrain (Rongali *et al*., 2018). To this end, LST maps prepared from satellite images are an attractive alternative as it provides a continuous dataset (Ogunode & Akombelwa, 2017).

LANDSAT 5 & 7

Land surface temperature was extracted using band 6 for Landsat 5 and 7 (Chen *et al*., 2020). Firstly, digital numbers (DNs) of band 6 were converted into radiation luminance using equation 3.

$$\text{Radiance} = \left[\frac{LMAX-LMIN}{QCALMAX-QCALMIN}\right](\text{QCAL} - \text{QCALMIN}) + \text{LMIN} \quad 3$$

Where QCALMIN is equal to 1, QCALMAX is equal to 255. QCAL stands for DN, in this case the thermal band (6), whereas LMAX and LMIN are equal to 1 and 255, respectively. LST in Kelvin was calculated using equation 4.

$$\text{T (K)} = K2/\ln\left(\frac{K1}{Yy} + 1\right) \quad 4$$

Values in Degree Celsius, 273.15 was subtracted from the result in equation 2.

$$\text{LST} = \text{T (K)} - 273.15 \quad 5$$

LANDSAT 8

To estimate the land surface temperature for Landsat 8, in ArcGIS 10.8, Map algebra, a feature in the spatial analyst tool which has the raster calculator in it was used in the five steps process:

i. Digital Numbers (DNs) were converted using equation 4 to Top of Air Atmosphere (TOA) spectral Radiance using the radiance rescaling factor provided in the metadata file

$$\text{L}\lambda = \text{MLQCAl} + \text{AL} \quad 6$$

where L_λ = Top of atmosphere spectral radiance, M_L = Radiance Multi Band for band 10 (0.0003342), A_L = Radiatiance Add Band for band 10 (0.1), Q_{CAL} = Band 10 (Digital Number)

ii. Conversion of Radiance into brightness temperature (T_B) which is the microwave radiance traveling upward from the top of Earth's atmosphere (Yang *et al*., 2014) using the thermal constants provided in the metadata file using equation 7:

$$\text{TB} = \text{K2/In}\left((\text{K1} / \text{L}\lambda) + 1\right) - 273.15 \quad 7$$

where K_1 = Calibration Constant 1 (774.8853), and K_2 = Calibration Constant 2 (1321.0789) all found in the metadata file.

iii. NDVI values were calculated using the equation 8.

$$NDVI = \frac{Float(NIR - RED)}{Float(NIR + RED)} \quad 8$$

iv. Derivation of the surface emissivity. To get the LSE, the PV (Proportion of vegetation) was first derived from NDVI of 2021 using the expression:

$$PV = \frac{(NDVI \quad - \quad NDVImin)}{(NDVImax \; - \; NDVImin)} \tag{9}$$

v. LST was calculated using the equation:

$$\mathrm{LST} = \mathrm{TB}/\,[1 + (\lambda * \mathrm{TB}/\rho) * \ln(\varepsilon)] \tag{10}$$

All calculations where done using raster calculator, a map algebra, spatial analyst tool in ArcGIS 10.8

2.6.1 LST Validation

To validate the accuracy of the estimated LST, a temperature based (T-Based) method was used. The T-based is a ground-based method that directly compares the satellite-derived LST with Insitu LST measurements at the satellite overpass (Li et al., 2013). The meteorological observatory data for temperature obtained from NIMET was compared with the LST estimated from Landsat thermal bands. Since the NIMET data was monthly, the temperature for the months that corresponds with the date of the Landsat imagery acquisition was compared using Microsoft excel and the result obtained were seen to be closely related.

2.7 Relationship between the Vegetation Loss and Land Surface Temperature

To assess the relationship between vegetation loss and LST, firstly, the total area in hectares occupied by classified vegetation for 1990, 2001 and 2021 and compared with the corresponding maximum retrieved LST values for 1990, 2001 and 2021 using the stacked bar chart. In addition to the above method, the relationship between vegetation loss and LST of the study area was equally assessed by comparing the vegetative index (NDVI) for each year and the LST for the corresponding year in ArcGIS 10.8. This was achieved by generating point data for NDVI and LST using fishnet polygon. Fishnet polygons, a sampling tool, under data management tools were created in ArcGIS 10.8. Thereafter, extraction was carried out by the tool 'Extract Multi Values to point' on both images (LST & NDVI) and the result was then clipped using the study area boundary shapefile to generate the result of Extract Multi Values to point for the LST and NDVI images. After this process, the multi values of points for LST and NDVI were exported from the attribute table of the clipped image and accessed in Microsoft excel. Here in excel, relationship between LST and NDVI for Bwari Area Council for the different study periods were determined through the use of scatter plot, assigning of a trendline to the graph and the derivation of r-squared values for the regression analysis. Similarly, the built-up index (NDBI) was compared with the LST for the years 1990, 2001 and 2021. This was done to determine the effect the increase in urbanization in the study area has made on the urban climate (LST).

3. Results and Discussion

The research focused on analyzing the impact of vegetation loss on Land Surface Temperature of Bwari Area Council through the mapping and analyzing the Landuse/Landcover between 1990 to 2021, assessing the spatio-temporal changes in the Land Surface Temperature of the study area, to the relationship that exist between the LST and the vegetation loss in the study area. The outcome of the data processing and analysis were presented in the form of maps and tables

3.1 Accuracy Assessment of LULC Classification

To determine the correctness of the land cover classification carried out for the study area and for the years under review, an assessment of the accuracy was carried out and shared in Tables 3, 4 and 5 which is the result of the assessment for years 1990, 2001 and 2021.

Table 3: Accuracy assessment for 1990 LULC Classification

Class(1990)	Water body	Built-up	Vegetation	Bare ground	Ground truth	Accuracy
Water body	27	0	0	0	27	100
Built-up	0	25	0	0	25	100
Vegetation	0	0	84	0	84	100

Bare ground	0	1	0	71	72	98.6
Total	27	26	84	71	208	
Producer Accuracy (%)	100	96.154	100	100		
Overall Accuracy	27+25+84+71=207	27+25+1+84+71=208	99.519			
Kappa Coefficient	0.993					

Table 4: Accuracy assessment for 2001 LULC Classification

Class(2001)	Water body	Built-up	Vegetation	Bare ground	Ground truth	Accuracy % (%))
Water body	31	0	0	0	31	100
Built-up	0	0	77	0	77	100
Vegetation	0	1	0	27	28	96.429
Bare ground	0	71	0	0	71	100
Total	31	72	77	27	207	
Producer Accuracy	100	98.611	100	100		
Overall Accuracy	31+77+27+71=206		31+77+2+1+71=207	99.51		
Kappa Coefficient	0.993					

Table 5: Accuracy assessment for 2021 LULC Classification

Class(2021)	Built-up	Water	Vegetation	Bare ground	Ground truth	Accuracy
Water body	62	0	0	1	63	98.413
Built-up	0	30	0	0	30	100
Vegetation	1	0	88	1	90	97.778
Bare ground	0	0	0	59	59	100
Total	63	30	88	61	242	
Producer Accuracy	98.413	100	100	96.721		
Overall Accuracy (%)	62+30+88+59=239	63+30+90+59=242	98.79			
Kappa Coefficient	0.983					

3.2 Land Use/Land Cover Change (LULCC) Analysis:

From the results of the analysis, it was observed that in 1990, rock/bare ground constituted the largest landcover for the study area occupying more than half of the total area at 43603(ha) which constitutes a percentage value of 57%, followed by vegetation occupying 30497(ha) which constitutes a percentage value of 40%, then built-up occupied only a small portion of the area at 1263(ha) making up 2% of the total space and finally the smallest was water body occupying only 866(ha) making up just 1% of the total study area.

From a close examination of the map in Figure 2, it can be observed that the dominant landcover class, rock/bare ground, was present in the entire study area with more concentration in the Northwest and central region. Vegetation was also prominent in the study area and mostly found in northeastern, eastern and western region with some concentration of vegetation found also in the south. There was very minimal built-up area in the study area as at 1990 but the few ones were settlements close to the rocks while water body was located at the bottom area of the central region. These results can be seen in Figures 2 and 3 which shows the Landuse Landcover map of 1990 and the observed patterns of 1990 in pie chart.

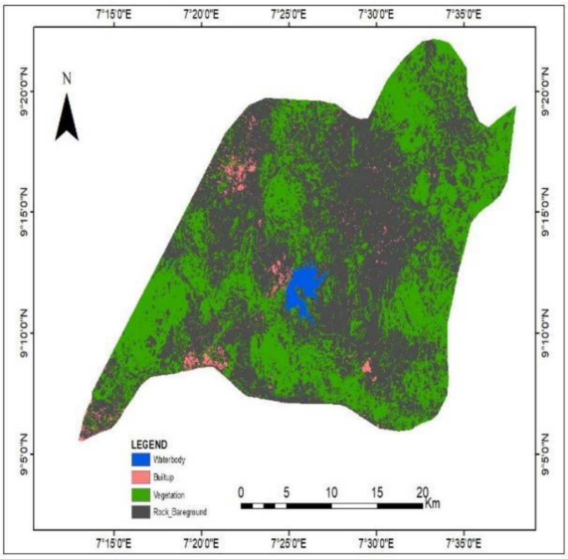

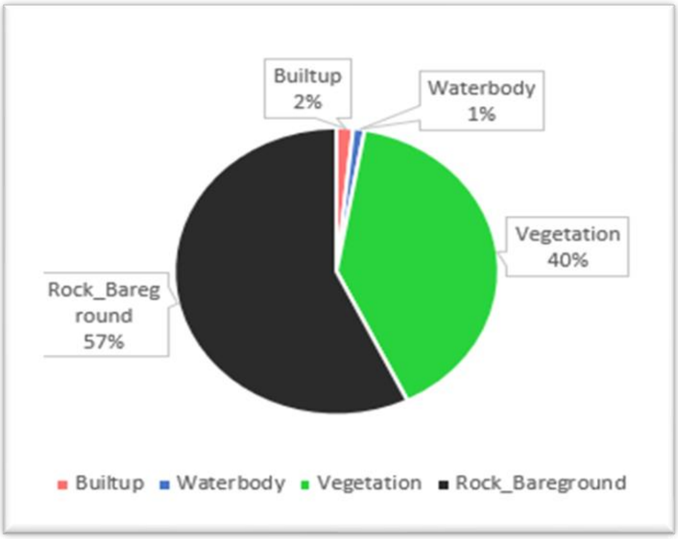

Figure 2: LULC 1990: Bwari Area Council **Figure 3:** Pictorial Representation of LULC class for 1990

According to similar analysis carried out in 2001, it was observed that due to increased farming activities, vegetation now increased from 30497(ha) to 37028(ha) now occupying 49% to become the largest landcover for the study area, followed by rock/bare ground occupying 31427(ha) at 41%, built-up now occupied 6898(ha) standing at 9% of the total coverage area and then water body occupying 875(ha) with a percentage of 1% was observed as the landcover class that occupied the smallest fraction of the study area. Observing the map, it can be seen that the dominant landcover class, vegetation, was present in the entire study area except for small portions in the north east and southern regions occupied by built-up. Rock/bare ground was observed more in the north across to the central region while water body maintained it position close to the central part of the study area.

These results can be seen overleaf in Figures 4 and 5 which shows the Landuse Landcover map of 2001 and the observed patterns of 2001 in pie chart

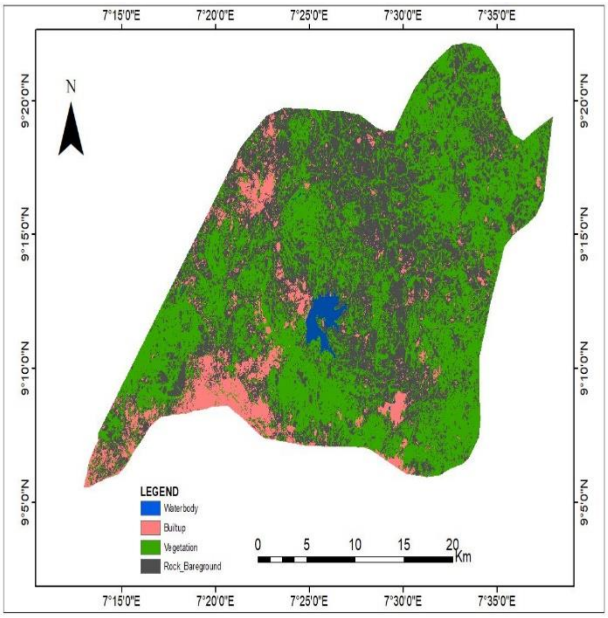

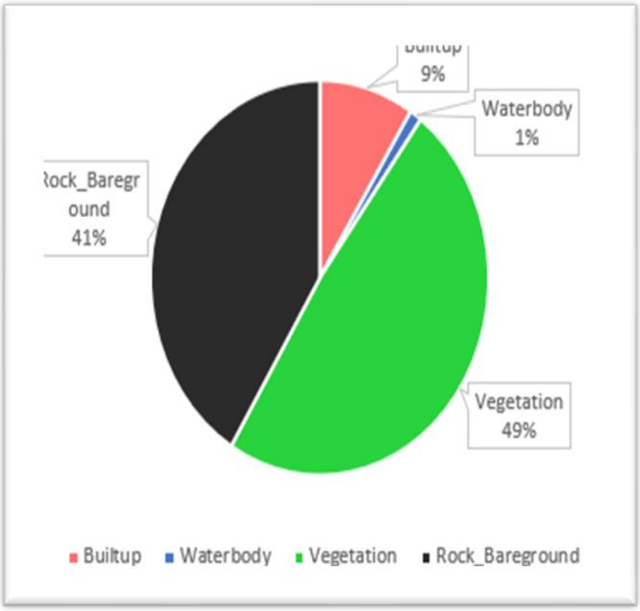

Figure 4: LULC 2001: Bwari Area Council **Figure 5:** Pictorial Representation of LULC class for 2 2001

Lastly, in 2021, as seen in Figures 6 and 7, built up became the largest land-cover occupying 35% of the study area on an area of 26808(ha), followed by rock/bare ground at 33% occupying 25436(ha), vegetation now occupied 22980(ha) at 30% and then the smallest land-cover class was water body occupying just 844(ha) to make 1% of the study area. Observing the map, it can be seen that dominant land-cover class in 2021, now the built-up area, occupied mostly the north western part of the study area connecting down to the southern region. The central region was occupied mostly by rocks/bare ground serving as a major hindrance to the spread of built-up to the area, vegetation was now more prominent in the north eastern part while water body still occupied its same position throughout the study period.

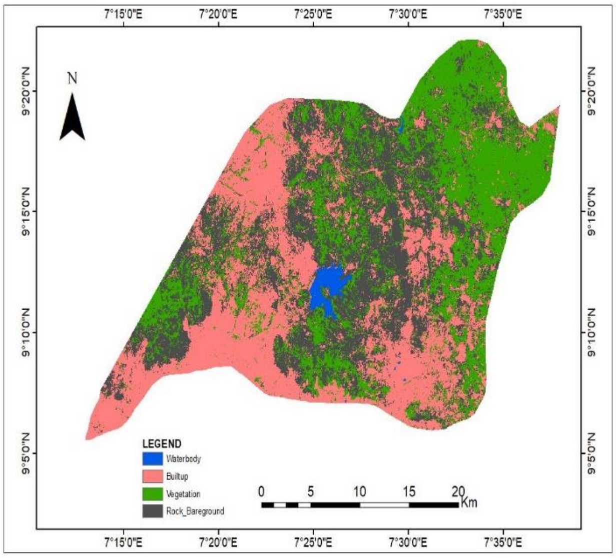

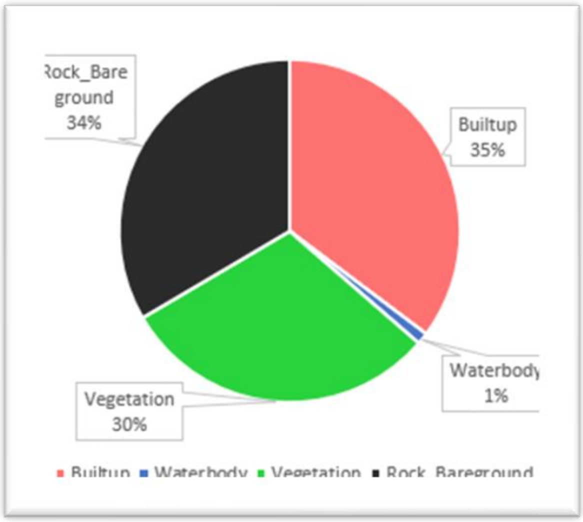

Figure 6: LULC 2021: Bwari Area Council **Figure 7:** Pictorial Representation of LULC class 2021

It is evidently clear that the expansion of the built-up area in Bwari Area Council from 1990 to 2021, has been to the detriment of vegetation, rock/bare ground and water body although the impact on the water body is minimal. A large expansion of the built-up area happened toward the north western region connecting with the central and southern part of the area council. Built-up area expansion towards the north eastern part of the area council is not so significant, and this is mostly due to the effect of the landscape of the area as it is mostly filled with rocks and hilly terrains. Table 6 gives a tabular representation.

Table 6: Areas of LULC for Bwari Area Council

Land use class	Changes btw 1990-2021(ha)	% changes	Changes btw 2001-2021(ha)	% changes	Changes btw 1990-2021(ha)	% changes

Built up	1263	1.66	6898	9.05	26808	35.24
Water body	866	1.14	875	1.15	844	1.11
Vegetation	30497	40.00	37028	48.58	22980	30.21
Bare ground	43603	57.20	31427	41.23	25436	33.44

To further identify the changes in the different Land-use/Land-cover classes that have occurred in the study area between the years under study, Table 7 overleaf shows the changes in the Land-use/Land-cover class between1990 to 2021. From the table, it can be observed that the highest percentage change in the classes, was observed in built-up between 1990-2021 with a 255% increase as compared to other periods between 1990-2001, and 2001-2021. Water body experienced minimal change between the study periods with the highest -0.31% between2001-2021. In vegetation, the highest percentage change was observed between 1990-2021(table7) with a change of -75.17% while the highest change in rock/bare ground was observed between 1990 and 2021 with a value of -181.67%. However, there was vegetation increase observed between1990 to 2001. This was due to the fact that in 1990, the study area was mostly filled with rocks and less human inhabitants and this made farming activities very low that year (lesser vegetation cover) and only picked up slowly after the Federal capital Territory was moved to Abuja in 1991 where the bare grounds had to now be cultivated and the rocks blasted as well to create expansion of agricultural lands to cater for the feeding of the increasing population of people relocating to Bwari.

Table 7: Percentage changes in Landuse/Landcover Classes between 1990-2021

Land use class	Changes btw 1990-2001(ha)	% changes	Changes btw 2001-2021(ha)	% changes	Changes btw 1990-2021(ha)	% changes
Built up	5635	56.35	19910	199.1	25545	**255.45**
Water body	9	0.09	-31	-0.31	-22	-0.22
Vegetation	6531	65.31	-14048	-140.48	-7517	**-75.17**
Bare ground	-12176	-121.76	-5991	-59.91	-18167	**-181.67**

3.3 Normalized Difference Vegetation Index (NDVI)

To generate Land Surface Temperature of the study area, NDVI maps had to be generated for the study area. Figures .8, 9 and 10 shows the results of the NDVI generated. From the maps, it can be seen that, in 1990, the vegetation in the study area can be classed as good and but was in few locations of the map. In 2001, the vegetation value though a positive in the maximum range (0.098), it is classed as not good, meaning that though vegetation was present, the density and greenness was very low. This value possibly indicates the presence of farmlands and its more concentrated in the south east end of the study area and a little into the south west. In 2021, the density of the vegetation has improved as compared to 2001 with a higher max value of 0.317. It is observed that areas that were greyish in color in 1990 and 2001 signifying low NDVI values now had deeper green colors in 2021. This areas in the previous years were occupied by rocks/bare ground but now in 2021, the rocks now nonexistent, have green areas in the locations. This explains why the vegetation density and greenness improved in 2021.

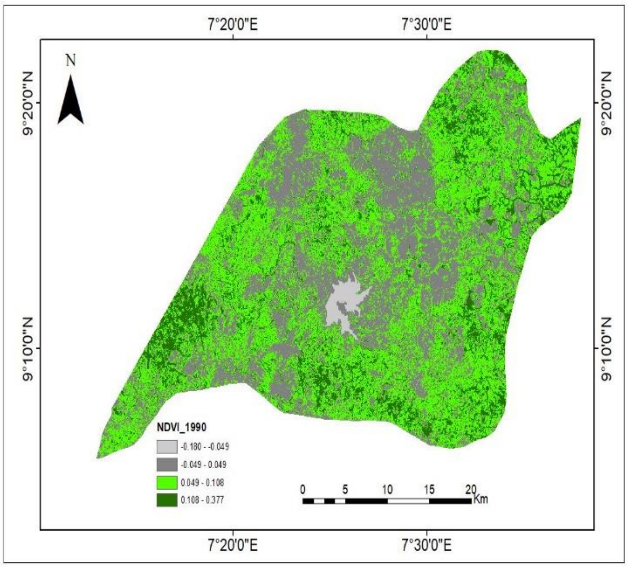

Figure 8: NDVI map for 1990

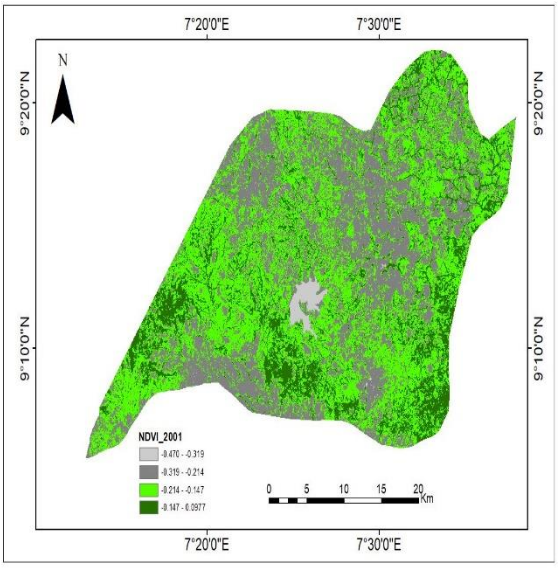

Figure 9: NDVI map for 2001

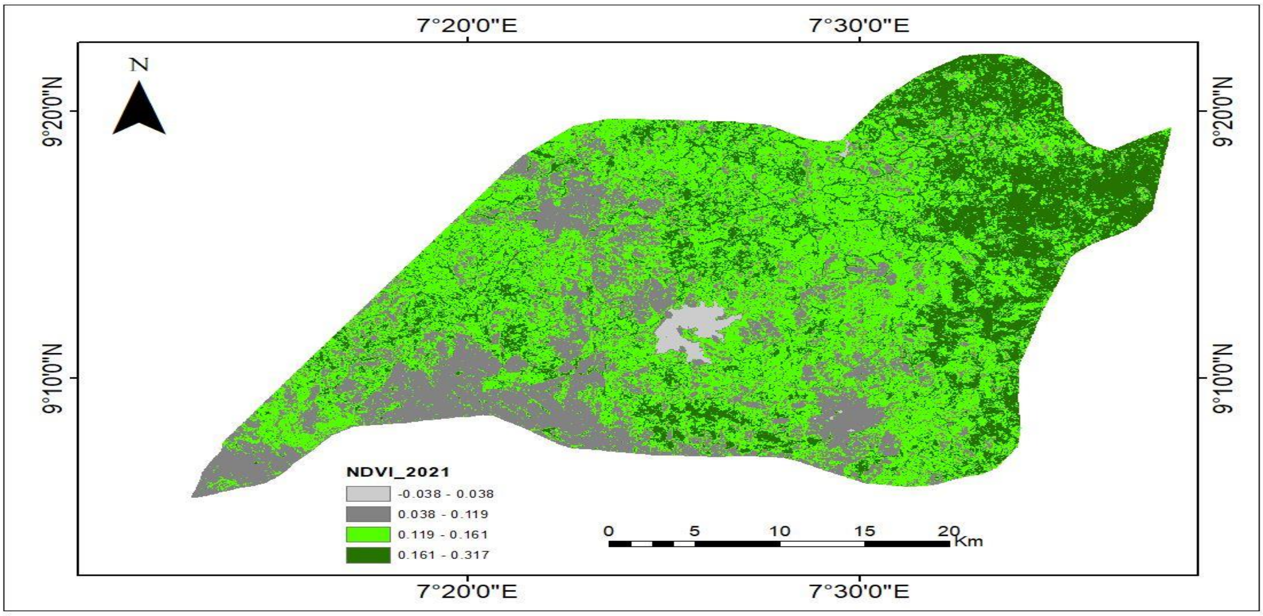

Figure 10: NDVI map for 2021

3.4 Land Surface Temperature Change Analysis

The result from the LST retrieved from the Landsat thermal bands is represented in Figures 11, 12 and 13 for 1990, 2001 and 2021 respectively. From the observation made from the LST maps, the temperature range was between 19.43^{0}C to 37.11^{0}C for 1990, 15.54^{0}C to 44.91^{0}C for 2001 and 21.96^{0}C to 58.87^{0}C. The maximum temperature increased by 21.77^{0}C between 1990 to 2021 while the minimum temperature increased by 2.53^{0}C. The point of the high maximum temperature observed in 2021, is a rocky mountain side located in the northern part of Mpape, a town in Bwari Area Council. This area is prominently filled with quarry site and there is a lot of mining of rocks by burning going on in the area. This explains why the LST levels is higher in that area as compared to other areas in the study area.

In comparing the LST map of 1990 with LULC map of 1990, it is observed that higher values of LST is more significant in the regions with deep red color and this corresponds to areas occupied mostly by rock/bare grounds, followed by built-up and lower in areas occupied by vegetation and water body in the LULC map.

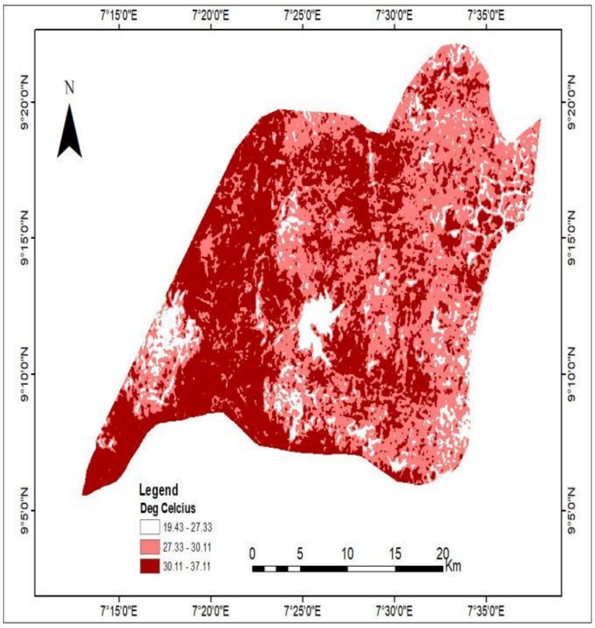

Figure 11: LST map for 1990

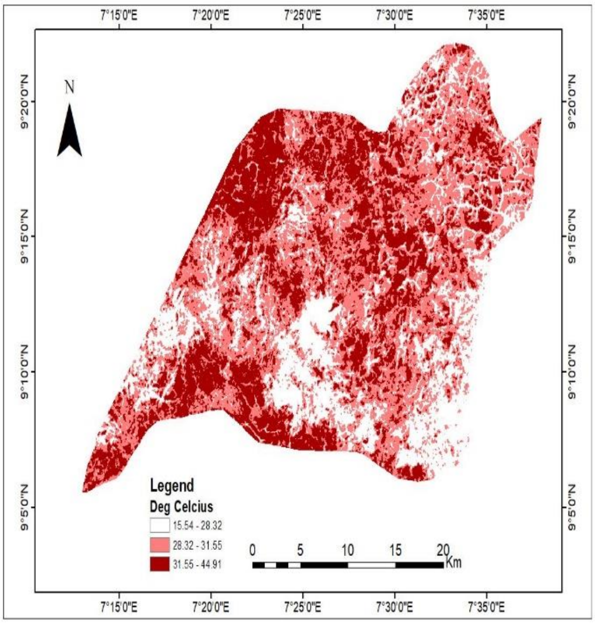

Figure 12: LST map for 2001

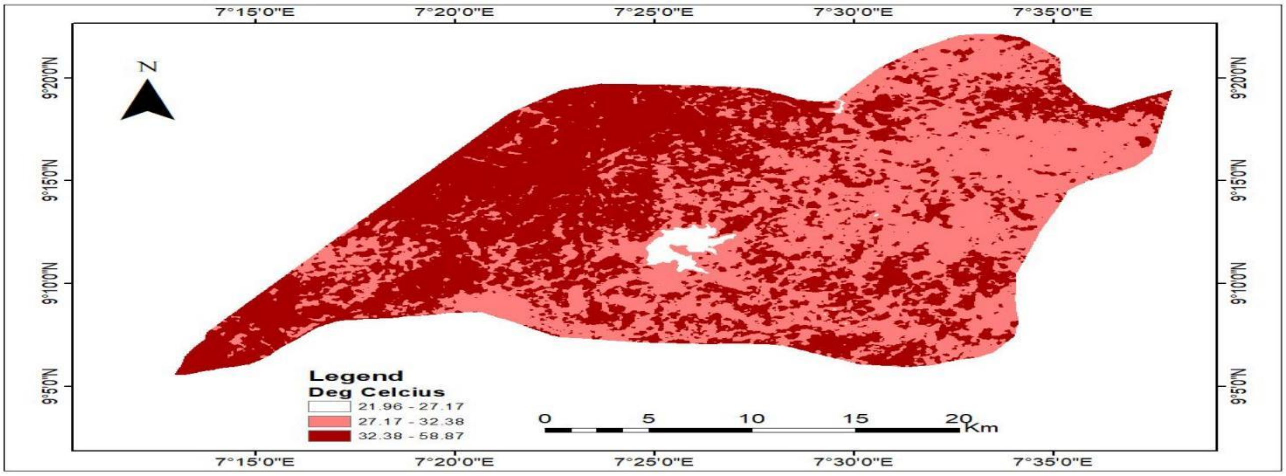

Figure 13: LST map for 2021

In LST map for 2001 (Figure 12), locations with bright red colors, signifying higher temperature (30.97-44.91⁰C) were found to be occupied equally by both rock/bare grounds and built-up and the spread of the high temperature was found to be distributed evenly across the study area except for the southeast region. Lowest temperature areas (15.54-27.75⁰C) were mostly found where vegetation was prominent and also areas occupied by water body this is attributed to the higher latent heat transfer and evapotranspiration properties of water body and vegetation (Yuan & Bauer, 2007).

3.5 LST Validation

LST obtained from Landsat 5, 7 and 8 was compared with the air temperature obtained from NIMET station located at Nnamdi Azikiwe international airport, Abuja Municipal Council (AMAC). NIMET data from single stations located at different Area Councils were used. The comparison made with air temperature, is usually different and can sometimes result in big differences since the resolution of the Landsat imageries for the used bands is high for the thermal bands (100 m for Landsat 8, 120m for Landsat 7 and 60m for Landsat 5, though all resampled to 30m) and 30 m for the red and NIR bands. Sometimes, the differences can be very big depending on the weather condition and other factors surrounding the weather station.

The result of this comparison is as represented in Figure 14.

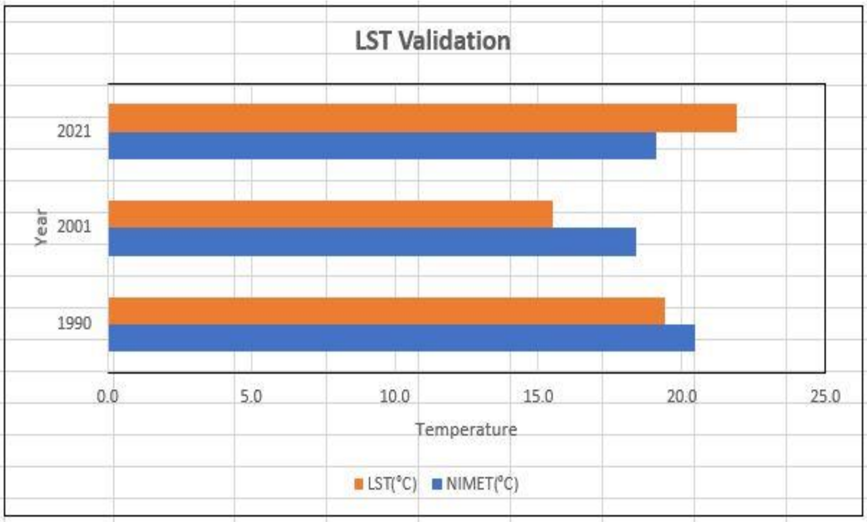

Fig 14: LST validation using NIMET data

From the results, LST was generally higher than temperature obtained from NIMET for 1990, 2001 and 2021 with 2001 recording the highest difference of 2.9°C. This difference is in close agreement to allowable difference 5⁰C as stated by Avdan & Jovanovska, (2016) that comparing LST results with the ground measurements results, may have an error up to 5⁰C. This makes the observed differences normal and expected.

3.6 Correlation Analysis between NDVI, NDBI and LST

The vegetation index NDVI for 1990, 2001 and 2021 was compared with LST of the corresponding years to show the relationship between the two variables. Similarly, LST was also compared with the built-up index (NDBI) to determine the impact of increase in built-up on the LST of the study area as shown in figure 15 to Figure 20.

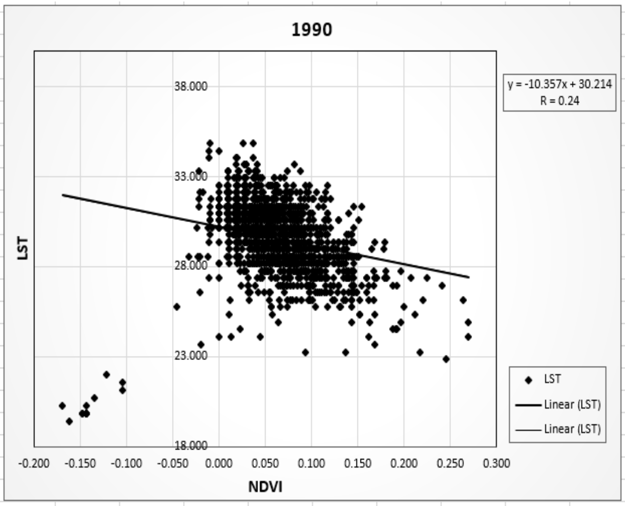

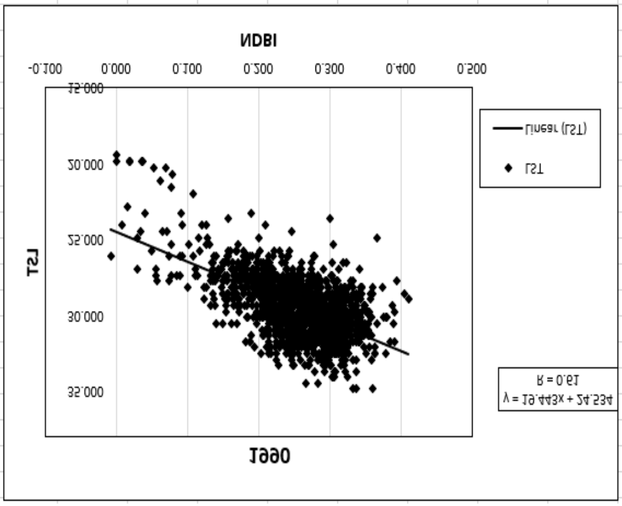

Figure 15: Correlation between NDVI and LST 1990 **Figure16:** Correlation between NDBI and LST 1990

A moderate negative correlation is notice (Figures 15 and 16) to exist between LST and NDVI in 1990 where r is equal to 0.24 and a strong positive relationship is found to exist between LST and NDBI where r is 0.61. This shows that land surface temperature is lower where vegetation index is high and LST is higher where NDVI values are lower. But with respect to NDBI, LST is higher as NDBI goes higher too.

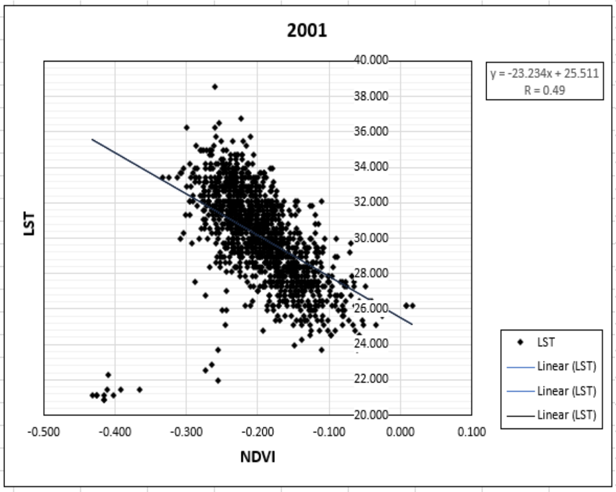

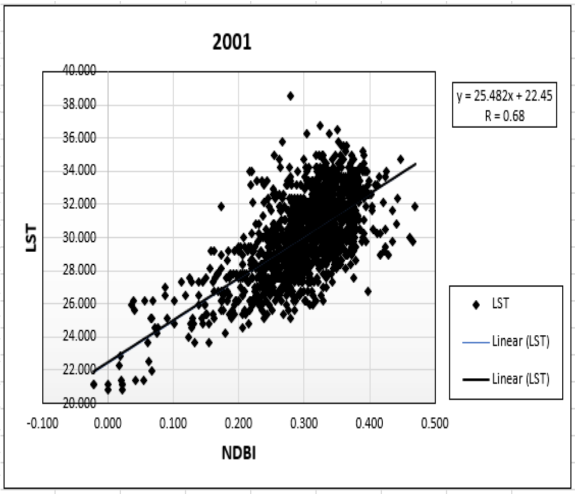

Figure 17: Correlation between NDVI and LST 2001 **Figure 18:** Correlation between NDVI and LST 2001

A moderate negative correlation is noticed, Figures 15 and 16 to exist between LST and NDVI where r is equal to 0.49 and high positive relationship exist between LST and NDBI with the value of r = 0.68. An increasing value of LST resulted in a decreasing value of NDVI (Figures 17 and 18) while as LST increased, NDBI increase as well. Figure 19: Correlation between NDVI and LST; 2021

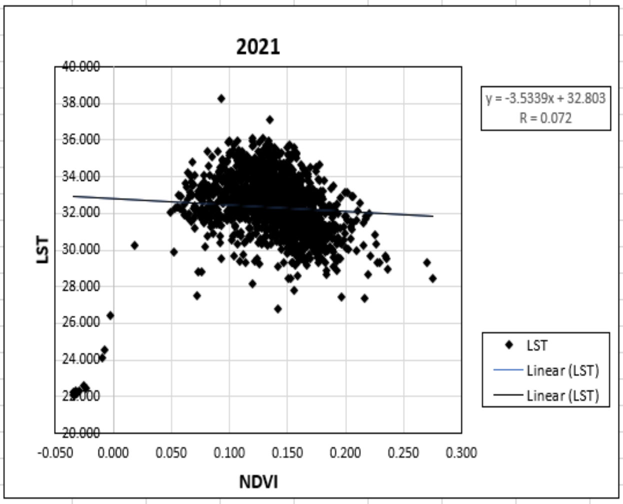

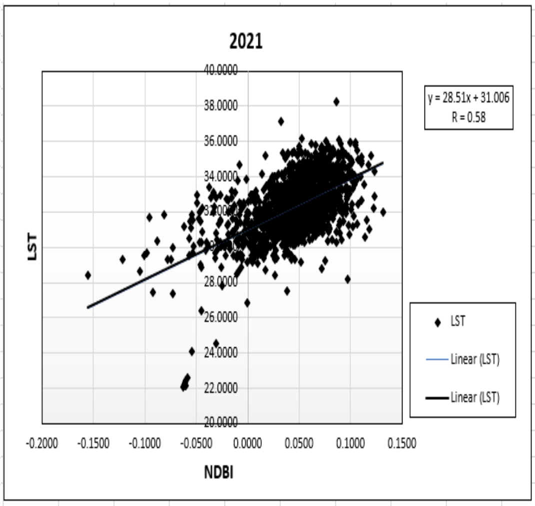

Figure 19: Correlation between NDVI and LST; 2021 **Figure 20:** Correlation between NDBI and LST; 2021

The correlation of LST with NDVI and NDBI in 2021 is shown in Figures 19 and 20. A very weak negative relationship was found between LST and NDVI with r equal to 0.072, whereas between LST and NDBI it was a moderate positive relationship with r equal to 0.58. According to these relationships, its noticed that the effect vegetation has on LST is not as high as the previous years due to less vegetation in the study area. However, in areas where vegetation exist, it was still noticed that higher NDVI lead to lower LST, and lower NDVI leads to higher LST. On the other hand, a positive relationship between LST and NDBI means that LST increases with NDBI increase and decreases with the decreasing NDBI. This correlation proves that urban vegetation contributes to a decrease in LST and can help to maintain thermal homogeneousness in cities while a loss of the vegetation leads to an increase in LST.

3.7 Relationship between Land Surface Temperature and Vegetation Loss between the Study Periods

To determine the relationship between vegetation loss and LST of Bwari Area Council over years 1990, 2001 and 2021, computed values for areas occupied by vegetation in the years under study was combined with the maximum LST values for the corresponding years. The result is presented in Figure 21.

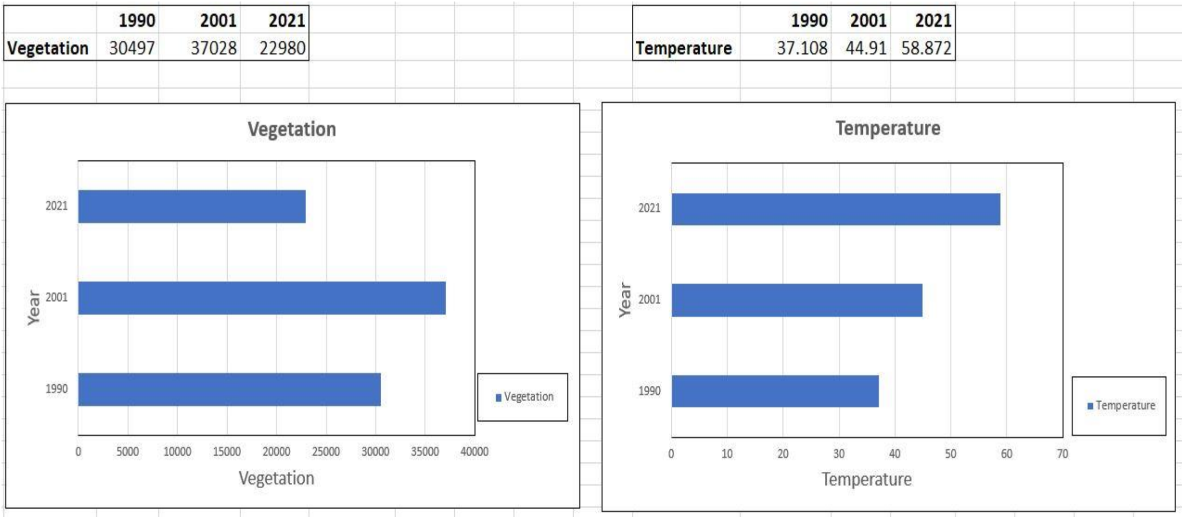

Figure 21: Relationship between vegetation loss and temperature between the study period.

It was observed that a decrease in vegetation experienced between 1990-2021(-7,517ha) was accompanied by an increase in LST (21.764^{0}C). However, between 1990-2001, there was an increase in vegetation but yet an increase in LST was observed. Further finding revealed that the LST in the study area has been increasing not only because of a loss in vegetation, but also due to the explosive rate of built-up and the exposure of rocks which is a prominent feature in the study area. These two components (built-up and rock) are known to have high emissivity levels thereby, rapidly increasing the LST of the area. So, from the above result, it can be deduced that though a loss in vegetation has had an impact in increasing the temperature between 1990-2021, this was not the only reason for the increase of LST in the study area. Further study is advised to be carried out to determine the effects that the increase in blasting of rocks, quarry activities and crude rock mining have on the LST of the study area.

3.8 Discussion of Findings

Between 1990 and 2001, built-up areas increased significantly from 1263ha to 6893ha (56.35%), obviously due to the expansion of residential areas in the satellite towns in Abuja to accommodate the daily increasing population of people moving to the capital city. During this period, more ministries were moved from Lagos to FCT to continue the transfer of capital headquarters and this led to obvious higher influx of people to the study area during this period. However, the increase in built-up surfaces wasn't accompanied with a loss in vegetation, as vegetation was observed to increase from 30497ha to 37028ha (65.67%). This increase is largely due to the increase in agricultural activities in the study area such as the increase of farmlands for the purpose of plant cultivation for feeding purposes. As a result of increase in agricultural activities and built-up areas, rock/bare ground reduced drastically from 43603ha to 31427ha (-121%). Within the same study period, water body increased slightly from 866ha to 875ha (0.09%). Similarly, maximum land surface temperature increased by 7.8^{0}C from 37.11˚C to 44.91˚C, while minimum temperature decreased by 3.89^{0}C from 19.43^{0}C to 15.54^{0}C. The value of 44.91˚C observed as the maximum temperature for 2001 and 15.54^{0}C as the minimum temperature in this study, is closely in agreement with maximum LST value of 45.1˚C and minimum value of 16.7 ˚C observed by Omali, (2020) in his study of the ecological evaluation of UHI impact in Abuja Municipal Council (AMAC).

In this study, the increase in the maximum temperature was due to the increased urbanization activity that went on during that period which lead to increase in anthropogenic activities and increase in impervious surfaces within the study period. Also exposed rock surfaces which by now is a common occurrence in the study area with low absorptivity, high emissivity and albedo properties, equally contributed to the increase in LST of the study area. From the relationship between NDVI, NDBI and LST for the period, results revealed that the increase in temperature over the period was due to increased impervious surfaces and loss of vegetative cover. Between 2001 and 2021, the built-up areas increased even more drastically from 6898ha to 26808ha (199.1%). The major contributor to this massive increase was the reduction of vegetation and rock/bare ground which reduced by 140.48% and 59.99% respectively.

During this period, the real estate sector experienced a boom as more houses were built to accommodate the fast-increasing population in some satellite towns in the area council such as Kubwa, Dutse, Bwari, Mpape etc. This invariably led to the increase of more impervious surfaces and subsequent loss of vegetation and rock/bare ground. The vegetation cover, cleared during the construction of buildings and infrastructure is not replaced after the development through landscaping in the study area, thus, resulting in discomfort from the increased surface temperature of the study area. Maximum temperature increased by 13.96°C from 44.91˚C to 58.87˚C while minimum temperature by 6.42°C from 15.54°C to 21.96°C. The findings from the NDVI and NDBI relationship with LST revealed that the increase in built-up area was accompanied with increase in land surface temperature while increase in vegetation was accompanied by decrease in land surface temperature.

4. Conclusion

The spatio-temporal LULC maps generated for the year 1990, 2001 and 2021 revealed notable changes in the study area in the last three decades. It was observed that due to rapid urbanization in the study area, built-up areas was the land cover type that increased the most from 1263ha to 26808ha (255.45%) while the rock/bare ground was the landcover type that reduced the most from 43603ha to 25436ha (181.67%) and these changes directly lead to increase in temperature within the study area over the last 30years.. This is connected to the expansion of real estates observed to be on the increase in the study area in the 30year period to accommodate the explosive population. The increased exposure of rocks through blasting and quarry activities was observed to significantly contributed to rise in temperature from a maximum 37.11°C to 58.87°C while the minimum temperature increased from 19.43°C to 21.96°C.The study also revealed 75.17% reduction in the vegetative cover, 255.45% increase in built-up, 181.67% reduction in rock/bare ground and 0.22% reduction in water body over the time period 1990 – 2021. The result of these changes is the corresponding increase in LST between 1990-2021 (21.764°C). Remote Sensing and Geospatial techniques used in this study has proven to be an effective method to be used in the study of Landuse and cover changes and its impact on the rise of land surface temperature of the study area.

References

Anker, Y., Mirlas, V., Gimburg, A., Zilberbrand, M., Nakonechny, F., Meir, I. and Inbar, M. 2019. Effect of rapid urbanization on Mediterranean karstic mountainous drainage basins. *Sustainable Cities* and *Society*, *51*: 101704.

Arsiso, B. K., Mengistu Tsidu, G., Stoffberg, G. H. and Tadesse, T. (2018). Influence of urbanization-driven land use/cover change on climate: The case of Addis Ababa, Ethiopia. *Physics and Chemistry of the Earth, Parts A/B/C*, *105*: 212–223. https://doi.org/10.1016/j.pce.2018.02.009

Avdan, U. and Jovanovska, G. 2016. Algorithm for Automated Mapping of Land Surface Temperature Using LANDSAT 8 Satellite Data. *Journal of Sensors*, *2016*: 1–8. https://doi.org/10.1155/2016/1480307

Awuh, ME., Japhets, PO., Officha, MC., Okolie, AO. and Enete, IC. 2019. A Correlation Analysis of the Relationship between Land Use and Land Cover/Land Surface Temperature in Abuja Municipal, FCT, Nigeria. *Journal of Geographic Information System*, *11*(01): 44–55. https://doi.org/10.4236/jgis.2019.111004

Ayanlade, A. and Howard, MT. 2019. Land surface temperature and heat fluxes over three cities in Niger Delta. *Journal of African Earth Sciences*, *151*: 54–66. https://doi.org/10.1016/j.jafrearsci.2018.11.027

Bachir, N., Bounoua, L., Aiche, M., Maliki, M., Nigro, J. and El Ghazouani, L. 2021. The simulation of the impact of the spatial distribution of vegetation on the urban microclimate: A case study in Mostaganem. *Urban Climate*, *39*: 100976. https://doi.org/10.1016/j.uclim.2021.100976

Balogun, IA. and Daramola, MT. 2019. The impact of urban green areas on the surface thermal environment of a tropical city: A case study of Ibadan, Nigeria. *Spatial Information Research*, *27*(1): 23–36. https://doi.org/10.1007/s41324-018-0219-6

Bowler, DE., Buyung-Ali, L., Knight, TM. and Pullin, AS. 2010. Urban greening to cool towns and cities: A systematic review of the empirical evidence. *Landscape and Urban Planning*, *97*(3): 147–155.

Chen, HC., Han, Q. and De Vries, B. 2020. Modeling the spatial relation between urban morphology, land surface temperature and urban energy demand. *Sustainable Cities and Society*, *60*: 102246. https://doi.org/10.1016/j.scs.2020.102246

Chibuike, EM., Ibukun, AO., Abbas, A. and Kunda, JJ. 2018. Assessment of green parks cooling effect on Abuja urban microclimate using geospatial techniques. *Remote Sensing Applications: Society and Environment*, *11*: 11–21. https://doi.org/10.1016/j.rsase.2018.04.006

Choudhury, D., Das, K. and Das, A. 2019. Assessment of land use land cover changes and its impact on variations of land surface temperature in Asansol-Durgapur Development Region. *The Egyptian Journal of Remote Sensing and Space Science*, *22*(2): Article 2. https://doi.org/10.1016/j.ejrs.2018.05.004

Di Leo, N., Escobedo, FJ. and Dubbeling, M. 2016. The role of urban green infrastructure mitigating land surface temperature in Bobo-Dioulasso, Burkina Faso. *Environment, Development and Sustainability*, *18*(2): 373–392. https://doi.org/10.1007/s10668-015-9653-y

Edicha, JA. and Mgbanyi, LLO. (n.d.). *Assessment of Soil Structural Stability Under Different Vegetal Cover Conditions In The Federal Capital Territory, Abuja, Nigeria*. *9*, 12.

Hami, A., Abdi, B., Zarehaghi, D. and Maulan, S. B. (2019). Assessing the thermal comfort effects of green spaces: A systematic review of methods, parameters, and plants' attributes. *Sustainable Cities and Society*, *49*: 101634.

Heather S. SussmanAjay RZ. 2019. Impact of increased urbanization on surface temperature, vegetation, and aerosols over Bengaluru, India, Remote Sensing Applications: Society and Environment, 16: 100266, https://doi.org/10.1016/j.rsase.2019.100261

Igun, E. and Williams, M. (2018). Impact of urban land cover change on land surface temperature. *Global Journal of Environmental Science and Management*, *4*(1). https://doi.org/10.22034/gjesm.2018.04.01.005

Kafy, A.-A., Al Rakib, A., Akter, KS., Rahaman, ZA., Faisal, AA., Mallik, S., Nasher, NMR., Hossain, MdI. and Ali, MdY. 2021. Monitoring the effects of vegetation cover losses on land surface temperature dynamics using geospatial approach in Rajshahi City, Bangladesh. *Environmental Challenges*, *4*: 100187. https://doi.org/10.1016/j.envc.2021.100187

Li, ZL., Tang, BH., Wu, H., Ren, H., Yan, G., Wan, Z., Trigo, IF. and Sobrino, JA. 2013. Satellite-derived land surface temperature: Current status and perspectives. *Remote Sensing of Environment*, *13:* 14–37. https://doi.org/10.1016/j.rse.2012.12.008

Macarof, P. and Statescu, F. 2017. Comparasion of NDBI and NDVI as Indicators of Surface Urban Heat Island Effect in Landsat 8 Imagery: A Case Study of Iasi. *Present Environment and Sustainable Development*, *11*(2): 141–150. https://doi.org/10.1515/pesd-2017-0032

Mahmoud, SH. and Gan, TY. 2018. Long-term impact of rapid urbanization on urban climate and human thermal comfort in hot-arid environment. *Building and Environment*, *142*: 83-100. https://doi.org/10.1016/j.buildenv.2018.06.007Get rights and content

Maimaitiyiming, M., Ghulam, A., Tiyip, T., Pla, F., Latorre-Carmona, P., Halik, Ü., Sawut, M. and Caetano, M. 2014. Effects of green space spatial pattern on land surface temperature: Implications for sustainable urban planning and climate change adaptation. *ISPRS Journal of Photogrammetry and Remote Sensing*, *89*: 59–66.

Mushore, TD., Mutanga, O., Odindi, J. and Dube, T. (2017). Linking major shifts in land surface temperatures to long term land use and land cover changes: A case of Harare, Zimbabwe. *Urban Climate*, *20*: 120–134. https://doi.org/10.1016/j.uclim.2017.04.005

Norton, BA., Coutts, AM., Livesley, SJ., Harris, RJ., Hunter, AM. and Williams, NS. 2015. Planning for cooler cities: A framework to prioritise green infrastructure to mitigate high temperatures in urban landscapes. *Landscape and urban planning*, *134*: 127-138. https://doi.org/10.1016/j.landurbplan.2014.10.018

NPC. 2006. National Population Commission (NPC)

Ogunode, A. and Akombelwa, M. 2017. An algorithm to retrieve Land Surface Temperature using Landsat-8 Dataset. *South African Journal of Geomatics*, *6*(2): 262. https://doi.org/10.4314/sajg.v6i2.10

Oliveira, S., Andrade, H. and Vaz, T. 2011. The cooling effect of green spaces as a contribution to the mitigation of urban heat: A case study in Lisbon. *Building and environment*, *46*(11): 2186-2194. https://doi.org/10.1016/j.buildenv.2011.04.034

Rakiya, AB., Halilu, AS., Mohammed, SO., Shagari, MS., Yusuf, MJ., Jagila, J. and Ajonye, ES. 2018. Assessing the Drivers of Vegetal cover dynamics in the FCT, Nigeria using remote sensing/GIS techniques. *International Journal of Environment, Agriculture and Biotechnology*, *3*(6): 2214–2221. https://doi.org/10.22161/ijeab/3.6.36

Rongali, G., Keshari, AK., Gosain, AK. and Khosa, R. 2018. Split-Window Algorithm for Retrieval of Land Surface Temperature Using Landsat 8 Thermal Infrared Data. *Journal of Geovisualization and Spatial Analysis*, *2*(2): 14. https://doi.org/10.1007/s41651-018-0021-y

Santamouris, M. 2014. Cooling the cities – A review of reflective and green roof mitigation technologies to fight heat island and improve comfort in urban environments. *Solar Energy*, *103*: 682–703. https://doi.org/10.1016/j.solener.2012.07.003

Sekertekin, A. and Bonafoni, S. 2020. Land Surface Temperature Retrieval from Landsat 5, 7, and 8 over Rural Areas: Assessment of Different Retrieval Algorithms and Emissivity Models and Toolbox Implementation. *Remote Sensing*, *12*(2): 294. https://doi.org/10.3390/rs12020294

Seto, K., Güneralp, B. and Hutyra, L. 2012. Global Forecasts of Urban Expansion to 2030 and Direct Impacts on Biodiversity and Carbon Pools. *Proceedings of the National Academy of Sciences*, *109*: 16083–16088. https://doi.org/10.1073/pnas.1211658109

Sharma, A., Conry, P., Fernando, HJS., Hamlet, AF., Hellmann, JJ. and Chen, F. (2016). Green and cool roofs to mitigate urban heat island effects in the Chicago metropolitan area: Evaluation with a regional climate model. *Environmental Research Letters*, *11*(6): 064004.

Shashua-Bar, L. and Hoffman, ME. (2000). Vegetation as a climatic component in the design of an urban street. *Energy and Buildings*, *31*(3): Article 3. https://doi.org/10.1016/S0378-7788(99)00018-3

Tran, H., Uchihama, D., Ochi, S. and Yasuoka, Y. 2006. Assessment with satellite data of the urban heat island effects in Asian mega cities. *International Journal of Applied Earth Observation and Geoinformation*, *8*(1): Article 1.

Ullah, S., Ahmad, K., Sajjad, RU., Abbasi, AM., Nazeer, A. and Tahir, AA. 2019. Analysis and simulation of land cover changes and their impacts on land surface temperature in a lower Himalayan region. *Journal of Environmental Management*, *245*: 348–357. https://doi.org/10.1016/j.jenvman.2019.05.063

Wang, YC., Hu, BKH., Myint, SW., Feng, CC., Chow, WTL. and Passy, PF. 2018. Patterns of land change and their potential impacts on land surface temperature change in Yangon, Myanmar. *Science of The Total Environment*, *643*: 738–750. https://doi.org/10.1016/j.scitotenv.2018.06.209

Waseem, S. and Khayyam, U. 2019. Loss of vegetative cover and increased land surface temperature: A case study of Islamabad, Pakistan. *Journal of Cleaner Production*, *234*: 972–983. https://doi.org/10.1016/j.jclepro.2019.06.228

Wuana, R., Ogbodo, C., Itodo, AU. and Eneji, IS. (2020). Ecological and Human Health Risk Assessment of Toxic Metals in Water, Sediment and Fish from Lower Usuma Dam, Abuja, Nigeria. *Journal of Geoscience and Environment Protection*, *08*(05): 82–106. https://doi.org/10.4236/gep.2020.85006

Yang, L., Cao, Y., Zhu, X., Zeng, S., Yang, G., He, J. and Yang, X. 2014. Land surface temperature retrieval for arid regions based on Landsat-8 TIRS data: A case study in Shihezi, Northwest China. *Journal of Arid Land*, *6*(6): 704–716. https://doi.org/10.1007/s40333-014-0071-z

Yuan, F. and Bauer, M. E. 2007. Comparison of impervious surface area and normalized difference vegetation index as indicators of surface urban heat island effects in Landsat imagery. *Remote Sensing of Environment*, *106*(3): 375–386. https://doi.org/10.1016/j.rse.2006.09.003